Direct Observation of Coherent Medium Response under the Condition of Two-Photon Excitation of Krypton by Femtosecond UV-Laser Pulses

O. Kittelmann,[1] J. Ringling,[1] A. Nazarkin,[2] G. Korn,[1] and I. V. Hertel[1]
[1]*Max-Born-Institut für Nichtlineare Optik und Kurzzeitspektroskopie, Rudower Chaussee 6, D-12489 Berlin, Germany*
[2]*P. N. Lebedev Physics Institute of the Russian Academy of Sciences, Leninsky Prospect 53, 117924 Moscow, Russia*
(Received 9 August 1995)

Coherent Rabi oscillations and subsequent phase relaxation of excitation were observed under the condition of two-photon resonant interaction of Kr atoms with intense femtosecond 193 nm laser pulses. The coherent dynamics of the atomic transition exposed to an intense field was resolved using the technique of fs-pulse four-wave mixing with probe pulses significantly shorter than the pump pulses.

PACS numbers: 42.50.Gy, 42.50.Md, 42.65.Ky

Since the first observation of coherent optical phenomena (e.g., self-induced transparency, optical nutation, photon echo, etc.), the resonant interaction of matter with laser pulses of duration τ_p short compared to the irreversible relaxation time T_2' of the medium polarization has become the subject of intensive studies, both theoretical and experimental. Phenomena arising from the coherent excitation of electric-dipole allowed transitions have been investigated in great detail [1].

Resonant and near-resonant two-photon excitations with ultrashort laser pulses of forbidden atomic transitions give access to an even wider class of nonlinear-optical processes such as two-photon absorption, stimulated Raman scattering, and four-wave sum- and difference-frequency mixing. The latter has proved to be a powerful tool for efficient femtosecond pulse generation in the vacuum ultraviolet (VUV) spectral range [2]. Nevertheless, up to now only a few experimental results have been obtained which allow the direct observation of the coherent dynamics in two-photon induced radiation-matter interactions (see experimental papers [3–6] and monograph [7]).

In this Letter we report for the first time a direct experimental observation of the coherent dynamics of an atomic two-photon excitation process using time-resolved four-wave difference-frequency mixing ($\omega_s = 2\omega_p \pm \omega_i$) with femtosecond UV and VUV pulses. Keeping the injected pulses (ω_i) significantly shorter than the pump pulses (ω_p) we were able to resolve Rabi oscillations and subsequent relaxation of the excitation at the probe difference frequency (ω_s). The results are of great importance for the understanding of coherent phenomena underlying the femtosecond VUV-pulse generation and further optimization of this process.

A two-photon transition has no dipole moment and coherent emission occurs only in the presence of an external field. This specific feature is exploited in coherent two-photon spectroscopy [3,4]. An additional field of frequency ω_i applied to a two-photon transition which had been excited by an intense pump pulse of frequency $\omega_p \cong \omega_{21}/2$ (ω_{21} being the frequency of the atomic transition) induces a coherent emission at the sum or difference frequency which allows one to probe the dynamics and coherence properties of the excited medium. With this technique, various processes which occur after the coherent two-photon excitation have recently been investigated (phase relaxation of an exciton polariton [3], ionization-initiated second harmonic generation [4], etc.). Previous experiments on two-photon resonant interaction of ultrashort pulses with atomic vapors [5,6] reported a pulse breakup into subpulses and an increase of transparency of the optically thick medium (the two-photon self-induced transparency effect [8]). These observations, however, give only indirect information about the state of the medium. Four-wave mixing has not been employed so far for a study of the dynamics of coherent radiation-atom interaction itself.

The pump and injected pulses used in the experiments were derived from the same fundamental output pulses of a 0.1 TW Ti:sapphire laser system (10 Hz repetition rate) by nonresonant sequential frequency mixing processes [9] which assured that they are perfectly synchronized on the femtosecond time scale. Stretching the 60 fs pulses from a self-mode-locked Ti:sapphire oscillator to 100 ps and subsequent amplification of these pulses in a Ti:sapphire laser system (chirped pulse amplification) leads to 8 mJ, 80 fs pulses at a wavelength of $\lambda = 774$ nm after recompression (stretcher-compressor design see Ref. [10]).

Tripling one part of the fundamental pulse by a cascaded sum-frequency mixing scheme (type I $\omega + \omega \rightarrow 2\omega$ and type II $2\omega + \omega \rightarrow 3\omega$) in two β-barium borate (BBO) crystals with lengths of 0.5 and 0.3 mm, respectively, provided 150 fs pulses at ω_i ($\lambda_i = 258$ nm). Quadrupling a second part of the fundamental pulses by sequential sum-frequency mixing (type I $\omega + \omega \rightarrow 2\omega$, type II $2\omega + \omega \rightarrow 3\omega$, type I $3\omega + \omega \rightarrow 4\omega$) in three BBO crystals resulted in 10 μJ, 193 nm seed pulses which were amplified to about 1.5 mJ by double passing an ArF gain module [11]. We employed a 0.5 mm long BBO crystal in the third mixing stage ($3\omega + \omega \rightarrow 4\omega$) which had an acceptance bandwidth

 0031-9007/96/76(15)/2682(4)$10.00

smaller than the spectral width of the incident radiation. Therefore only a part of the incident spectrum can contribute effectively to the frequency mixing process, thus leading to spectrally narrowed ($\Delta\lambda = 0.2$ nm) and temporally lengthened pulses at 193 nm. Using a cross-correlation technique [9] the temporal width (FWHM) of the amplified 193 nm pulses was measured to be 550 fs. Pumping with these pulses and probing with the 3 times shorter injection pulses (ω_i) made it possible to resolve the Rabi oscillations which are induced by the strong two-photon interaction of the pump pulses with the atomic medium. By varying the angle of the BBO crystal the center frequency of our 193 nm seed pulses was tunable within the bandwidth of the ArF gain profile. Thus we were able to excite the $4p^6\,{}^1S_0 \rightarrow 6p[5/2]_2$ two-photon transition in krypton. Exact resonance was verified by generating a maximum yield of the 123.6 nm fluorescence line of Kr and measuring the wavelength of the pump pulses. A relative measure of the energy at the difference frequency was determined by integration over the spectrum which was recorded with a charge coupled device detector after being properly filtered through a 0.2 m VUV monochromator.

Using Ar and Kr as nonlinear media two qualitatively different pictures of the medium response behavior have been observed. In Ar where the frequency detuning from the nearest two-photon resonance was large ($\approx$700 cm^{-1}) compared to the pump pulse spectral width $\Delta\omega_p$($\approx$55 cm^{-1}) a noticeable difference-frequency signal was observed only when the pump and the injected pulse overlapped each other in time. The corresponding dependence of the signal on the delay time represented a shape directly related to that of the pump pulse intensity (see Fig. 1, solid line).

In contrast, for two-photon excitation of Kr the dependence of the signal on the delay time shows a slow decay (Fig. 1) and a signal could be detected for delays as long as 20–30 ps. With an increase of gas pressure the decay time decreased monotonically. We also observed an oscillating substructure in the region where the pump and the injected pulse had a substantial temporal overlap. The substructure appeared only at pump pulse energies exceeding a critical value of 70–80 μJ corresponding to a fluence of 0.35–0.4 J/cm^2 (2×10^{-4} cm^2 focal spot size). The characteristic time scale of these oscillations became shorter and the number of peaks increased with increasing pump pulse energy [Fig. 2(a)].

We explain these results by a model of two-photon resonant frequency mixing using pulses short compared to the polarization relaxation time T_2' [12]. The difference-frequency signal is proportional to the injected pulse intensity multiplied by a factor determined by the two-photon medium response. For the nonresonant Ar case the medium response follows quasistationary the pump pulse intensity [13]. In the resonant case of Kr coherent Rabi oscillations are observed within the pump pulse duration followed by free relaxation of the excitation due

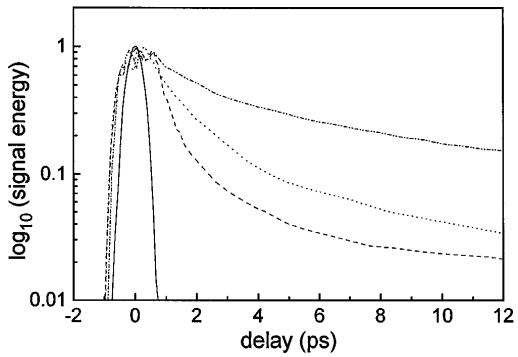

FIG. 1. Measured pulse energy of the difference-frequency signal at ω_s as a function of the delay between the pump (ω_p) and the injected (ω_i) pulses in Ar (solid line, $p =$ 80 mbar) and Kr (dashed line, $p = 500$ mbar; dotted line, $p =$ 120 mbar; dashed +2 dots, $p = 25$ mbar) with $E_p = 450$ μJ and $\tau_p = 550$ fs.

to Doppler (T_D^*) and collisional (T_2') broadening which is significantly longer than the pump pulse duration τ_p (see estimates below).

We now give a more quantitative explanation of the experimental results. In the general case the solution of the coupled evolutionary equations for the density matrix σ_{mn} of the resonant transition and the Maxwell equations for the complex amplitudes E_p, E_i, E_s of the interacting pulses is required [7,12]. However, the analysis of the equations can be simplified for the following reasons: First, experimentally the estimated two-photon absorption length at the pump pulse frequency considerably exceeds the active region length ($L_a \sim 1$ cm) so that propagation effects can be neglected; second, the intensities of the injected and generated pulses are considerably lower than that of the pump pulse, and therefore the dynamics of the resonant interaction in both Ar and Kr is mainly determined by the pump pulse. Because no intermediate levels occur in Ar and Kr close to a one-photon resonance with the injected and the generated field carrier frequencies the phase velocity mismatch of the interacting fields is estimated to be not too large to affect the difference-frequency generation. Within the above approximations the temporal behavior of the generated field intensity after the propagation of the length z is given by [12]

$$|E_s(z,\tau)|^2 \propto |E_i(\tau - \Delta\tau)|^2 |\langle\sigma_{12}(\tau)\rangle|^2. \qquad (1)$$

In Eq. (1) $\tau = t - z/c$ is the retarded time; $E_i(\tau - \Delta\tau)$ describes the temporal shape of the injected pulse amplitude, where $\Delta\tau$ accounts for the time delay of the pulse with respect to the pump pulse field $E_p(\tau)$ centered at $\tau = 0$. The time evolution of the off-diagonal density matrix element σ_{12} is determined by solving the equations for a two-level atom interacting with the pump field $E_p(\tau)$ [8,13],

$$\frac{\partial\sigma_{12}}{\partial\tau} = -i\Delta\Omega\sigma_{12} - i\frac{g}{4\hbar}nE_p^{*2} - \frac{\sigma_{12}}{T_2'}, \qquad (2a)$$

$$\frac{\partial n}{\partial\tau} = 4\mathrm{Im}\left\{\frac{g}{4\hbar}E_p^2\sigma_{12}\right\} - \frac{n+1}{T_1}, \qquad (2b)$$

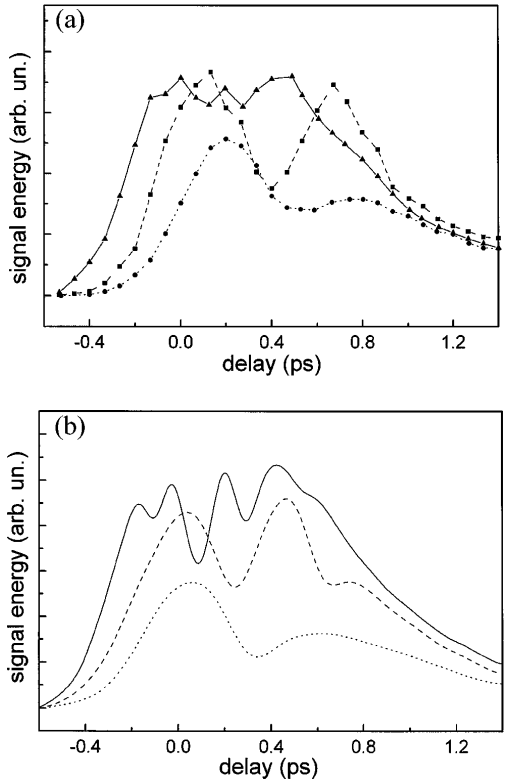

FIG. 2. (a) Measured pulse energy of the difference-frequency signal as in Fig. 1 for short delay times within the pump pulse duration (550 fs) using 150 fs injected pulses and a Kr pressure of 250 mbar. The pump pulse energies were 100 μJ (dotted line + circles), 200 μJ (dashed line + squares), and 450 μJ (solid line + triangles). (b) Results of numerical model calculation according to Eq. (2) for Kr with the pump pulse parameters $\tau_p = 550$ fs, $E_p = 100$ μJ (dots), 200 μJ (dashes), 450 μJ (solid line), and $p = 250$ mbar and taking into account the Gaussian transverse beam profile. The corresponding pump pulse parameters $W(\infty)$ at the beam axis are 2.3π, 4.6π, and 10.4π.

where $n = \sigma_{22} - \sigma_{11}$ is the population difference of the resonant levels, g the matrix element of the two-photon transition, $\Delta\Omega = \Delta\omega + \Delta\omega_{\mathrm{st}}$ the full nonstationary frequency detuning with the first term $\Delta\omega = \omega_{21} - 2\omega_p$ and the second term $\Delta\omega_{\mathrm{st}} = (\alpha_1 - \alpha_2)|E_p|^2/4\hbar$ accounting for the dynamical Stark shift of the resonant levels proportional to the level polarizabilities α_1 and α_2 [8,13]. The macroscopic medium response $\langle\sigma_{12}\rangle$ is obtained by the averaging of σ_{12} over the Doppler line contour g: $\langle\sigma_{12}\rangle = \int_{-\infty}^{\infty} g(\Delta\omega)\sigma_{12}(\Delta\omega)d\Delta\omega$. The Doppler dephasing time T_D^* in both gases is estimated to be $T_D^* \sim 100$ ps. When estimating T_2', we have to take into account that the highly excited upper resonant levels lie in the vicinity of the Rydberg states where the collision cross section of an atom sharply increases. Using theoretical calculations [14], the cross section of a Kr atom excited to the upper resonant $6p$ level is estimated to be $\sigma = 10^{-12}$ cm^2. This leads to $T_2' \sim 10^3$ ps$/p$ [mbar] due to the enlarged cross section and for gas pressures $p < 1$ bar the condition $\tau_p < T_2'$ of coherent interaction between the pump pulse and the two-photon transition is fulfilled. For the transition $4p^6\,{}^1S_0 \rightarrow 6p[5/2]_2$ in Kr we have resonant excitation since $|\Delta\omega| < \Delta\omega_p \approx \tau_p^{-1}$. Analysis of spectroscopic data [15] shows that the energy difference between the resonant $6p[5/2]_2$ level and the nearest upper $6p[3/2]_1$ and lower $6p[1/2]_1$ lying levels allowed for two-photon excitation is about 200 cm^{-1} and exceeds both the pump pulse spectral width ($\Delta\omega_p \approx 55$ cm^{-1}) and the dynamical Stark shift ($\Delta\omega_{\mathrm{st}} \leq 40$ cm^{-1}) of the resonant transition frequency. This justifies the two-level model described by Eq. (2).

Setting $\Delta\omega = 0$ in Eq. (2) and neglecting the relaxation terms during the interaction, for a pump pulse field free of phase modulation one can find a solution of Eq. (2) (see [8]) that leads to the following expression for the generated pulse intensity:

$$|E_s(z,\tau)|^2 \propto \left\{\frac{2\gamma^2[1 - \cos W(\tau)] + \sin^2 W(\tau)}{(1 + \gamma^2)^2}\right\} \times |E_i(\tau - \Delta\tau)|^2, \quad (3)$$

with

$$W(\tau) = \frac{g}{2\hbar}(1 + \gamma^2)^{1/2}\int_{-\infty}^{\tau}|E_p(\tau')|^2 d\tau'. \quad (4)$$

Equations (3) and (4) show that the measured signal as a function of $\Delta\tau$ is modulated with the Rabi frequency $\Omega_{\mathrm{Rabi}} = g(1 + \gamma^2)^{1/2}|E_p(\tau)|^2/2\hbar$, and with an increase of the pump pulse intensity $|E_p|^2$ the modulation frequency also increases. The factor $\gamma = (\alpha_1 - \alpha_2)/2|g|$ accounts for the contribution of the dynamical Stark shift. At the time interval $\tau > \tau_p$ the response relaxes according to $|\sigma_{12}(\tau)| \propto \exp\{-\tau^2/T_D^{*2} - \tau/T_2'\}$ [4]. The fact that with an increase of gas pressure the decay time decreases (Fig. 1) indicates that collisional relaxation predominates. Using the measured dependence we estimated the collision cross section by the value $\sigma \cong 2 \times 10^{-12}$ cm^2.

In Fig. 2(b) we present the results of model calculations based on the numerical solution of Eq. (2) for a gas pressure $p = 250$ mbar (corresponding to $T_2' \cong 1.5$ ps) and pump pulse energies of 100, 200, and 450 μJ using two-photon transition parameters estimated from [15] ($g = 2.1 \times 10^{-24}$ cm^3, $\alpha_1 - \alpha_2 = 5.8 \times 10^{-24}$ cm^3) and taking into account the transverse beam profile. The results are seen to be in qualitative agreement with the measured data and show that the averaging over the transverse beam profile and the effect of a finite temporal resolution flatten the modulations of the atomic response. Even for pulses with a maximum energy of 450 μJ the field-induced broadening due to fast Rabi oscillations was still smaller ($\sim$150 cm^{-1}) than the energy separation between the upper neighboring levels. The validity of the two-level model is supported by the fact that even in this extreme regime the characteristic oscillating structure appeared experimentally only within the interaction time. But there was no signal modulation at the stage

of free relaxation of the excitation (which would indicate excitation of other levels).

We have found that the critical energy density for the observation of Rabi oscillations in our case ($\gamma > 1$) is determined by the requirement that the Rabi angle $W(\infty)$ [see Eq. (4)] at the beam axis must exceed the value $W(\infty) = 2\pi$ [as can be seen qualitatively from Eq. (3)]. In this situation the population difference and the response $|\sigma_{12}|$ make one complete oscillation. The corresponding pump pulse critical fluence was calculated to be 0.35 J/cm^2 which is also in good agreement with our observations.

According to our estimates, the photoionization rate of the Kr atom from the upper resonant level was an order of magnitude smaller than the Rabi frequency because of a considerable reduction of ionization cross section σ_i for photon energies far above the ionization energy (we estimate σ_i by 10^{-19} cm^2 that gives for $I_p \sim 1$ TW/cm^2 an ionization rate of $\sim 5 \times 10^{11} s^{-1}$, whereas $\Omega_{\mathrm{Rabi}} \sim 10^{13}$ s^{-1}) so that ionization had a little effect on the process.

In conclusion, we have shown that fs-pulse four-wave frequency mixing makes it possible to study the coherent dynamics of a quantum transition in an intense resonant field. With this technique, the two-photon resonant response of atomic Ar and Kr excited by an intense VUV pulse with duration short compared to the polarization relaxation time was investigated. In Ar the frequency detuning from the two-photon transition is sufficiently large and the response of the medium shows quasistationary behavior determined by the instant value of the pump pulse field. In the resonant Kr case coherent Rabi oscillations and subsequent free relaxation of the excitation have been observed. These results are the first direct experimental observation of the coherence induced by a two-photon excitation of an atomic medium by femtosecond VUV pulses. The measured difference-frequency signal probes the squared amplitude of the off-diagonal matrix element of the transition. Such information about the dynamics of quantum transitions is of prime importance for controlling and optimizing such processes as two-photon resonant frequency conversion and harmonic generation, as well as time-resolved studies of Rydberg states in atoms and molecules.

We would like to acknowledge Professor D. J. Kaup and Dr. H. Steudel for the interest in our work and fruitful discussions. A. N. acknowledges the support by the Alexander von Humboldt Stiftung.

[1] L. Allen and J. H. Eberly, *Optical Resonance and Two-Level Atoms* (Wiley, New York, 1975).
[2] J. H. Glownia, D. R. Gnass, and P. P. Sorokin, J. Opt. Soc. Am. B **11**, 2427 (1994); A. Tünnermann, K. Mossavi, and B. Wellegehausen, Phys. Rev. A **46**, 2707 (1992).
[3] F. Vallee, F. Bogani, and C. Flytzanis, Phys. Rev. Lett. **66**, 1509 (1991).
[4] C. S. Mullin, D. Kim, M. B. Feller, and Y. R. Shen, Phys. Rev. Lett. **74**, 2678 (1995).
[5] N. Tan-no, K. Yokoto, and H. Inaba, Phys. Rev. Lett. **29**, 1211 (1972).
[6] N. P. Garayantz, V. S. Grigoryan, S. A. Michaelian, K. B. Petrossian, and K. M. Pokhsrarian, J. Mod. Opt. **38**, 591 (1991).
[7] J. F. Reintjes, *Nonlinear Optical Parametric Processes in Liquids and Gases* (Academic Press, London, 1984).
[8] E. M. Belenov and I. A. Poluektov, Sov. Phys. JETP **29**, 29 (1969).
[9] J. Ringling, O. Kittelmann, F. Noack, G. Korn, and J. Squier, Opt. Lett. **18**, 2035 (1993).
[10] J. V. Rudd, G. Korn, S. Kane, J. Squier, G. Mourou, and P. Bado, Opt. Lett. **18**, 2044 (1993).
[11] J. Ringling, O. Kittelmann, F. Noack, U. Stamm, J. Kleinschmidt, and F. Voss, Opt. Lett. **19**, 1639 (1994).
[12] I. A. Poluektov and A. V. Nazarkin, J. Quantum. Electron. **9**, 1495 (1979).
[13] D. Grischkowsky, M. M. T. Loy, and P. F. Liao, Phys. Rev. A **12**, 2514 (1975).
[14] E. W. McDaniel, J. B. A. Mitchell, and M. E. Rudd, in *Atomic Collisions, Heavy Particles Projectiles* (Wiley, New York, 1993).
[15] M. Aymar and M. Coulombe, At. Data Nucl. Data Tables **21**, 537 (1978).